Neurobiology of Aging 81 (2019) 138–145

Contents lists available at ScienceDirect

Neurobiology of Aging

journal homepage: www.elsevier.com/locate/neuaging

Cross-sectional associations between [^{18}F]GTP1 tau PET and cognition in Alzheimer's disease

Edmond Teng [a,*,1], Michael Ward [a,1], Paul T. Manser [b], Sandra Sanabria-Bohorquez [c], Rebecca D. Ray [c,d], Kristin R. Wildsmith [e], Suzanne Baker [c,g], Geoffrey A. Kerchner [a], Robby M. Weimer [f]

[a] Early Clinical Development, Genentech, Inc., South San Francisco, CA, USA
[b] Biostatistics, Genentech, Inc., South San Francisco, CA, USA
[c] Clinical Imaging Group, Genentech, Inc., South San Francisco, CA, USA
[d] Early Clinical Development Informatics, Genentech, Inc., South San Francisco, CA, USA
[e] Biomarker Development, Genentech, Inc., South San Francisco, CA, USA
[f] Department of Biomedical Imaging, Genentech, Inc, South San Francisco, CA, USA
[g] Molecular Biophysics and Integrated Bioimaging, Lawrence Berkeley National Laboratory, Berkeley, CA, USA

ARTICLE INFO

Article history:
Received 11 February 2019
Received in revised form 28 May 2019
Accepted 30 May 2019
Available online 6 June 2019

Keywords:
Tau
PET
Cognition
Alzheimer's disease
Clinical trial

ABSTRACT

The regional relationships between tau positron emission tomography (PET) imaging and cognitive impairment in Alzheimer's disease (AD) remain uncertain. We examined cross-sectional associations between cognitive performance, cerebral uptake of the novel tau PET tracer [^{18}F]GTP1, and other neuroimaging indices ([^{18}F]florbetapir amyloid PET, magnetic resonance imaging) in 71 participants with normal cognition, prodromal AD, or AD dementia. Greater [^{18}F]GTP1 uptake was seen with increasing clinical severity and correlated with poorer cognition. [^{18}F]GTP1 uptake and cortical volume (but not [^{18}F]florbetapir uptake) were independently associated with cognitive performance, particularly within the temporal lobe. Delayed memory was more specifically associated with temporal [^{18}F]GTP1 uptake; other domains correlated with a broader range of regional [^{18}F]GTP1 uptake. These data confirm that [^{18}F]GTP1 tau PET uptake significantly correlates with cognitive performance in AD, but regional correlations between performance in non-memory cognitive domains were less specific than reported by tau PET imaging studies that included participants with atypical focal cortical AD syndromes. Tau PET imaging may have utility as a surrogate biomarker for clinical AD progression in therapeutic trials of disease-modifying interventions.

1. Introduction

Over the past two decades, novel techniques for brain imaging in Alzheimer's disease (AD) have expanded our ability to identify specific forms of neuropathology in living individuals. In particular, PET imaging agents that bind amyloid-β (Aβ) plaques can identify significant cortical Aβ plaque deposition in symptomatic and presymptomatic individuals with underlying AD pathology (Villemagne et al., 2018). Aβ PET can be used in clinical settings, for clarifying differential diagnosis, and in clinical trials, as an inclusion criterion (to identify significant cerebral Aβ deposition) and as an outcome measure (for interventions targeting Aβ) (Villemagne et al., 2018).

Aβ plaques are one key pathological feature of AD; neurofibrillary tangles (NFTs) comprising hyperphosphorylated tau aggregates are another (Querfurth and LaFerla, 2010). Postmortem studies have shown that NFT density correlates more closely with neurodegeneration and cognitive impairment than Aβ plaque density (Nelson et al., 2012). Thus, tau PET imaging agents that bind to NFTs represent potential AD biomarkers that may correlate more closely with disease progression than Aβ PET.

The most widely studied tau PET tracer is [^{18}F]flortaucipir (also known as [^{18}F]AV-1451 or [^{18}F]T807) (Johnson et al., 2016; Pontecorvo et al., 2017; Schöll et al., 2016). AD-associated aggregated tau deposits identified by [^{18}F]flortaucipir demonstrate regional patterns that are consistent with postmortem neuropathological studies (Braak and Braak, 1991). Although significant correlations have been reported between [^{18}F]flortaucipir PET

Neurobiology of Aging https://www.elsevier.com/journals/neurobiology-of-aging/0197-4580?generatepdf=true.

* Corresponding author at: Early Clinical Development, Genentech, Inc, 1 DNA Way, South San Francisco, CA 94080. Tel.: +650-467-1661; fax: +650-467-2887.
E-mail address: teng.edmond@gene.com (E. Teng).

[1] Co-first authors.

0197-4580/$ – see front matter © 2019 Elsevier Inc. All rights reserved.
https://doi.org/10.1016/j.neurobiolaging.2019.05.026

signal and cognition across different cohorts (Bejanin et al., 2017; Brier et al., 2016; Cho et al., 2016; Johnson et al., 2016; La Joie et al., 2018; Maass et al., 2018; Mattsson et al., 2017; Ossenkoppele et al., 2016; Pontecorvo et al., 2017; Schöll et al., 2016; Schwarz et al., 2016), there have been some inconsistencies across studies. Cognitive performance has been shown to correlate with [^{18}F]flortaucipir PET signal: (1) across the entire cortex (Mattsson et al., 2017; Pontecorvo et al., 2017), (2) either across the entire cortex or with specific cortical regions in an assessment-depending fashion (Brier et al., 2016; Cho et al., 2016), (3) only in specific cortical regions (Bejanin et al., 2017; Johnson et al., 2016; Ossenkoppele et al., 2016), or (4) not at all (Koychev et al., 2017). Therefore, additional explorations of the correlations between tau PET signal and cognition in AD with other tau PET ligands could provide further evidence supporting the utility of tau PET for assessing AD severity.

[^{18}F]GTP1 (also known as [^{18}F]G02941054, [^{18}F]MNI-798, and [^{18}F]RO6880276) is a novel radiopharmaceutical under development for imaging tau aggregates in vivo. [^{18}F]GTP1 selectively binds to tau pathology in AD. It demonstrates significant uptake (suggesting substantial tau deposition) in AD subjects but no uptake in cognitively normal (CN) controls. The preclinical and clinical characterization of [^{18}F]GTP1 has been described in detail elsewhere and supports its utility as a tau PET tracer in AD (Sanabria-Bohorquez et al., 2019).

In this study, we tested the hypothesis that regional patterns of tau deposition are closely related to cognitive deficits in individual cognitive domains, which has primarily been supported by tau PET studies in cohorts that include participants with atypical focal cortical variants of AD who may have clinical presentations that are less representative of typical late-onset amnestic AD (Bejanin et al., 2017; Ossenkoppele et al., 2016). We examined relationships between performance on global and domain-specific cognitive instruments with global and regional [^{18}F]GTP1 signal in a cohort that mirrors the inclusion criteria for current clinical trials in AD (i.e., amnestic deficits, Aβ positive by PET). We also sought to confirm and extend prior work examining cross-sectional relationships between tau PET signal, Aβ PET signal, cerebral atrophy, and cognitive performance (Bejanin et al., 2017) across a spectrum of clinical AD severity.

2. Methods

2.1. Study design

We analyzed baseline data from an observational study designed to evaluate longitudinal change in tau burden using [^{18}F]GTP1 PET imaging in CN controls and participants with AD (GN30009; NCT02640092). These data included cognitive assessments, [^{18}F]GTP1 PET, Aβ PET using [^{18}F]florbetapir, and structural MRI. Baseline data from different subsets of this cohort have also been included in other analyses (Blennow et al., submitted; Sanabria-Bohorquez et al., 2019; Wildsmith et al., in preparation).

2.2. Participants

Participants age 50–85 years were enrolled from 11 research centers, which independently developed strategies for recruiting participants with normal cognition or amnestic AD (per local regulatory guidelines) that fulfilled all applicable inclusion and exclusion criteria outlined in the study protocol. Inclusion criteria for the CN group included absence of subjective cognitive complaints, absence of concerns for cognitive dysfunction from the study partner and investigator, global Clinical Dementia Rating (CDR) (Morris, 1997) of 0, and Mini–Mental State Examination (MMSE) (Folstein and McHugh, 1975) scores of 28–30. All participants in AD subgroups were required to have [^{18}F]florbetapir Aβ PET scans adjudicated as positive via visual read (Joshi et al., 2012) by two central raters and brain MRI scans that were consistent with AD and did not show significant non-AD neurological disease that might contribute to cognitive impairment.

Participants with prodromal AD met National Institute on Aging-Alzheimer's Association core clinical criteria for mild cognitive impairment (Albert et al., 2011) and had a global CDR of 0.5 and MMSE scores of 24–30. Participants with mild or moderate AD dementia met National Institute on Aging-Alzheimer's Association core clinical criteria for probable AD dementia, with an amnestic presentation (McKhann et al., 2011). Mild AD participants had a global CDR of 0.5 or 1 and MMSE scores of 22–30. Moderate AD participants had a global CDR of 0.5, 1, or 2 and MMSE scores of 16–21.

This study was approved by each research center's Institutional Review Board and was conducted in accordance with International Conference on Harmonization E6 Guidelines for Good Clinical Practice. Written informed consent was obtained for all participants and/or their legally authorized representatives in accordance with federal and institutional guidelines.

2.3. Neuropsychological testing

Baseline cognitive assessments included the MMSE, CDR, 13-item version of the Alzheimer's Disease Assessment Scale–Cognitive Subscale (ADAS-Cog13) (Mohs et al., 1997) and Repeatable Battery for the Assessment of Neuropsychological Status (RBANS) (Randolph et al., 1998). The CDR was analyzed using the Sum of Boxes (CDR-SB; range 0–18, higher scores indicate greater impairment). Total scores were used to analyze the MMSE (range 0–30, lower scores indicate greater impairment) and ADAS-Cog13 (range 0–85, higher scores indicate greater impairment). The RBANS was analyzed using total index scores (range 40–160, lower scores indicate greater impairment), which are adjusted for age. Raw scores from individual RBANS subtests were also analyzed.

2.4. [^{18}F]GTP1 PET imaging

[^{18}F]GTP1 was prepared at Invicro (New Haven, CT) as previously described (Sanabria-Bohorquez et al., 2019). [^{18}F]GTP1 PET scans were performed at a central imaging center (Invicro; New Haven, CT). [^{18}F]GTP1 images were acquired over a 30-minute window 60 minutes after injection after a mean (SD) bolus injection of 343 ± 31 MBq on Siemens HR+ PET or Biograph 6 PET-CT cameras. Images were reconstructed with an iterative reconstruction algorithm (OSEM 4 iterations, 16 subsets) and a post hoc 5 mm Gaussian filter to insure consistent image quality and data quantification between scanners as demonstrated from Hoffman phantom studies. Individual PET frames were motion-corrected and an average [^{18}F]GTP1 image was created, which was coregistered to MRI using attenuation correction CT when images were acquired in the PET-CT scanner. MRI was then spatially normalized to standard Montreal Neurological Institute space using SPM12 (www.fil.ion.ucl.ac.uk/spm/software/spm12), and normalization parameters were applied to the corresponding average [^{18}F]GTP1 image.

Composite regions of interest (ROIs) included the whole cortical gray matter (WCG) and an AD-signature temporal meta-ROI (voxel-number–weighted average of the average uptake in the entorhinal, amygdala, parahippocampal, fusiform, inferior temporal, and middle temporal ROIs; Jack et al., 2017). MRI tissue segmentation was performed to define cortical gray matter, and the Hammers atlas (Hammers et al., 2003) was used to define the temporal meta-ROI. Individual Hammers atlas ROIs were also used to examine for

correlations between specific brain regions and RBANS subtests. Separate analyses were performed for each ROI using [^{18}F]GTP1 signal from the left and right hemispheres, as well as [^{18}F]GTP1 signal averaged across both hemispheres. All [^{18}F]GTP1 standardized uptake value ratios (SUVRs) were calculated using inferior cerebellar gray as reference (Morris, 1997) and did not undergo partial volume correction.

[^{18}F]GTP1 has a high affinity and selectivity for tau pathology; in ex vivo studies, no measurable binding to Aβ plaques, MAO-B, or other tested proteins was seen (Sanabria-Bohorquez et al., 2019). In a subset of CN and AD participants, SUVR images in the 60–90 minute interval showed a slightly elevated signal in the putamen and globus pallidus that did not affect analyses of [^{18}F]GTP1-specific binding in cortical ROIs.

2.5. [^{18}F]florbetapir PET imaging

[^{18}F]florbetapir was prepared at commercial facilities, and Aβ PET imaging was performed on different scanners at different imaging centers associated with individual sites per manufacturer's instructions (Eli Lilly; Indianapolis, IA). Briefly, each participant underwent 20 minutes (4 frames, 5-minute duration) of serial PET imaging starting 50 minutes (±5 minutes) after injection. [^{18}F]florbetapir SUVR was calculated using the whole cerebellum as reference in both the WCG and temporal meta-ROI. Image reconstruction harmonization between scanners was performed using Hoffman phantom studies.

2.6. Magnetic resonance imaging

MRI was performed at individual research centers on different 1.5 T (27% of MRI images) or 3T (73% of MRI images) scanners for participant eligibility, and 3D sagittal T1-weighted magnetization-prepared rapid gradient-echo sequences were collected using the manufacturer recommended acquisition parameters for volumetric analyses and [^{18}F]GTP1 and [^{18}F]florbetapir PET image processing. Images were collected with 1 mm^2 in-plane resolution, 1.0–1.2 mm slice thickness, 256 mm × 256 mm matrix, and a 240 mm FOV. MRI/PET image processing was performed using SPM12. Cortical segmentation was performed using FreeSurfer version 6.0 (http://freesurfer.net) to measure cortical volumes in the WCG and temporal meta-ROI.

2.7. Statistical methods

Statistical analyses were performed using the R software package (v.3.3.2) (R Core Team, 2016). Baseline demographic, cognitive, and neuroimaging indices were compared between diagnostic groups using one-way analyses of variance for continuous measures and chi-squared tests for categorical variables. Post hoc analyses were performed using Tukey's test. Cross-sectional associations were evaluated between indices of tau burden (mean [^{18}F]GTP1 SUVR across the WCG or temporal meta-ROI), indices of Aβ burden (mean [^{18}F]florbetapir SUVR across the WCG or temporal meta-ROI), and cognitive performance at screening/baseline using Spearman correlations. Spearman partial correlations were used to assess relationships of cognitive performance with tau PET signal while adjusting for Aβ PET signal and with Aβ PET signal while adjusting for tau PET signal. Multiple linear regression models were used to assess the relative and combined variance in cognition explained by [^{18}F]GTP1 SUVR, [^{18}F]florbetapir SUVR, MRI cortical volumes, and age. Cross-sectional associations were also evaluated between [^{18}F]GTP1 SUVR in individual Hammers atlas ROIs and performance on individual RBANS subtests. These exploratory correlational analyses were adjusted for multiple comparisons using Benjamini-Hochberg correction for a false discovery rate of 0.05.

3. Results

3.1. Patient characteristics

Seventy-one participants who enrolled in the study from March 2016 to November 2017 had imaging and cognitive data available for analysis (Table 1). The diagnostic groups were similar in age, racial/ethnic background, and gender distribution (all $p > 0.1$). With increasing disease severity, progressively lower MMSE and RBANS scores and progressively higher CDR-SB and ADAS-Cog13 scores were seen (all $p < 0.001$). Likewise, progressively higher [^{18}F]GTP1 WCG SUVRs and progressively lower cortical volumes were seen (both $p < 0.001$). Greater [^{18}F]florbetapir WCG SUVR values were seen in AD groups than in the CN group, but mean [^{18}F]florbetapir WCG SUVR values did not differ across the three AD groups. Within the CN group, 3/10 participants were Aβ positive per visual read of Aβ PET scans. These participants were included in the study to allow for the analysis of [^{18}F]GTP1 signal across a broad spectrum of AD severity. The most common reason for screen failure in the AD groups was a [^{18}F]florbetapir PET scan adjudicated as Aβ negative.

3.2. [^{18}F]GTP1 PET imaging

Our previous work demonstrates that [^{18}F]GTP1 PET signal reflects the expected spatial distribution of tau pathology in AD for each corresponding disease stage (Sanabria-Bohorquez et al., 2019). Fig. 1A shows representative axial [^{18}F]GTP1 images for participants

Table 1
Baseline demographic, cognitive, and neuroimaging characteristics of study cohort

	CN (n = 10)	Prodromal AD (n = 27)	Mild AD (n = 19)	Moderate AD (n = 15)	*p*
Age	67.2 (6.2)	69.1 (7.5)	70.3 (6.1)	70.3 (7.0)	0.65
Sex (% male)	40%	48%	42%	60%	0.71
Race/ethnicity (% non-Hispanic white)	90%	96%	84%	88%	0.56
MMSE	29.2 (0.8)[a]	28.1 (1.4)[a]	26.0 (2.6)[b]	17.3 (3.0)[c]	<0.001
CDR-SB	0.0 (0.2)[a]	1.6 (0.8)[b]	3.3 (1.6)[c]	6.6 (2.1)[d]	<0.001
ADAS-Cog13	9.3 (5.0)[a]	14.7 (5.5)[a]	21.7 (6.8)[b]	39.2 (6.8)[c]	<0.001
Total RBANS	93.0 (10.8)[a]	86.2 (11.1)[a]	71.8 (14.0)[b]	55.3 (9.0)[c]	<0.001
WCG [^{18}F]GTP1 SUVR	1.18 (0.18)[a]	1.37 (0.15)[a]	1.40 (0.14)[b]	1.43 (0.16)[b]	<0.001
WCG [^{18}F]florbetapir SUVR	1.19 (0.18)[a]	1.20 (0.14)[b]	1.39 (0.14)[b]	1.41 (0.16)[b]	0.002
WCG volume (cm^3)[e]	418.9 (23.9)[a]	421.0 (32.4)[a]	397.8 (33.1)[a]	366.5 (28.8)[b]	<0.001

Data are expressed as means (SD). *p*-values refer to overall one-way ANOVA or chi-square tests.
[a-d]For indices with significant overall group effects, groups denoted by different letters differ by $p < 0.05$ by Tukey's test; groups denoted by the same letter are not significantly different from each other after correction for multiple comparisons. [e]Volumetric MRI data for 9 participants (8 prodromal, 1 mild AD) were not available for analysis.
Key: ADAS-Cog13 = 13-item version of the Alzheimer's Disease Assessment Scale-Cognitive Subscale; ANOVA = analysis of variance; CN = cognitively normal; CDR-SB = Clinical Dementia Rating Sum of Boxes; MMSE = Mini–Mental State Examination; RBANS = Repeatable Battery for the Assessment of Neuropsychological Status; SUVR = standardized uptake value ratios; WCG = whole cortical gray matter.

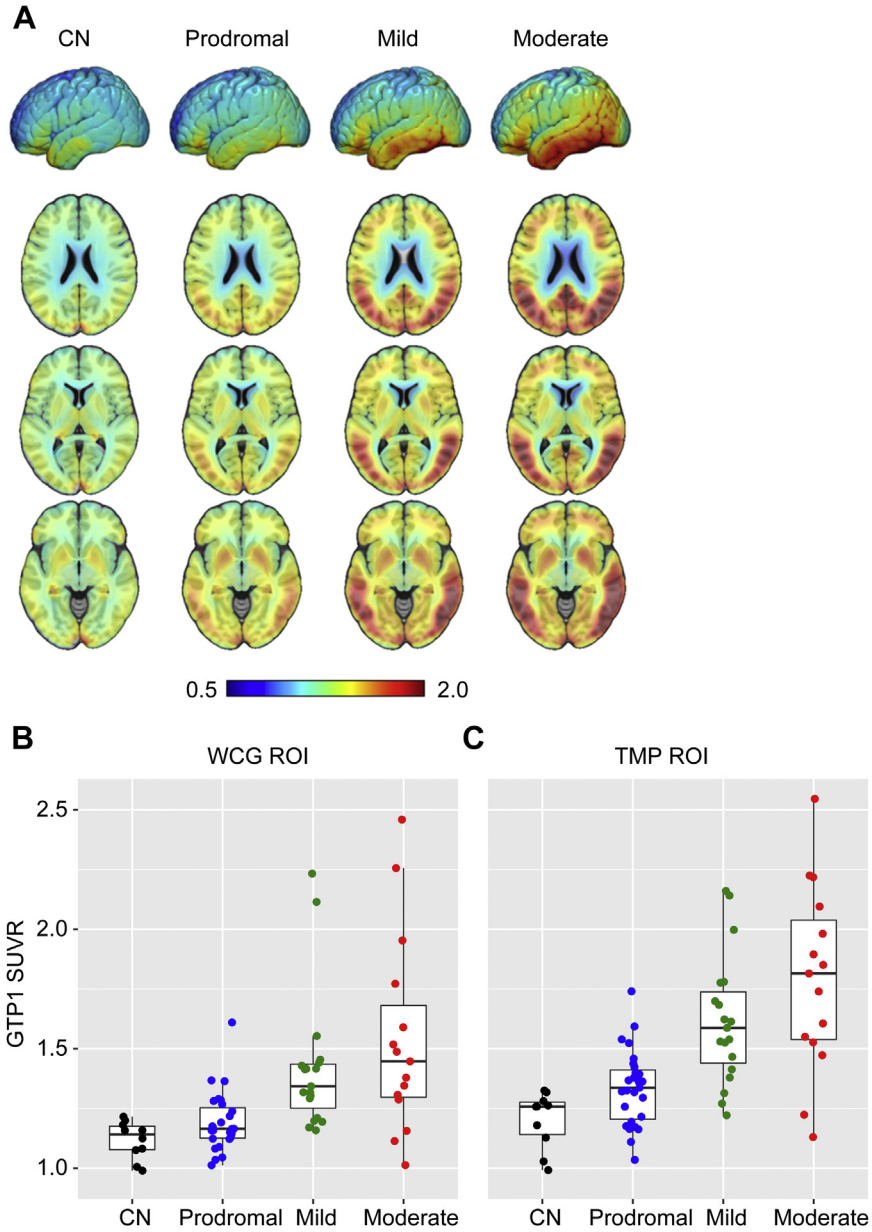

Fig. 1. Average baseline [^{18}F]GTP1 SUVR for cognitively normal (CN) participants and those with prodromal, mild, and moderate AD (A). Boxplots of [^{18}F]GTP1 SUVR data across diagnostic groups from the whole cortical gray matter (WCG) ROI (B) and temporal (TMP) meta-ROI (C). Abbreviations: AD = Alzheimer's disease; SUVR = standardized uptake value ratio; ROI = region of interest.

in each group. Progressively greater SUVRs in the WCG (Fig. 1B) and temporal meta-ROI (Fig. 1C) were seen with advancing disease severity. Similar to prior imaging studies with [^{18}F]flortaucipir (Pontecorvo et al., 2017; Schöll et al., 2016), there was some heterogeneity in the tau PET signal across diagnostic groups, including in the moderate AD group. The two moderate AD participants with the lowest [^{18}F]GTP1 SUVRs in the temporal meta-ROI had the highest MMSE scores (both 21/30) in that diagnostic group.

3.3. Correlations between WCG [^{18}F]GTP1 SUVR, WCG [^{18}F] florbetapir SUVR, and cognition

We initially examined correlations between cognitive performance across the entire study cohort with WCG [^{18}F]GTP1 or [^{18}F] florbetapir SUVR (Table 2). Although both tau ([^{18}F]GTP1) and Aβ ([^{18}F]florbetapir) PET signal significantly correlated with poorer performance on the MMSE, CDR-SB, ADAS-Cog13, and RBANS (all $p < 0.01$), Spearman's correlation coefficients were numerically larger with [^{18}F]GTP1 than [^{18}F]florbetapir, particularly when analyses were restricted to the temporal meta-ROI. We subsequently performed partial correlation analyses, adjusting [^{18}F]GTP1 WCG SUVR correlations for [^{18}F]florbetapir WCG SUVR (Supplemental Fig. 1A) and adjusting [^{18}F]florbetapir WCG SUVR correlations for [^{18}F]GTP1 WCG SUVR (Supplemental Fig. 1B). Although correlations between tau PET signal and cognition remained significant after adjusting for Aβ PET signal, none of the cognitive correlations with Aβ PET signal survived adjustments for tau PET signal.

Because all CN participants had normal cognition (per inclusion criteria) and most (7/10) had negative [^{18}F]florbetapir PET scans, and all AD participants had both impaired cognition and positive [^{18}F]florbetapir PET scans (also per inclusion criteria), the participant selection process may have biased our analyses toward

Table 2
Spearman correlations between global cognitive indices and [^{18}F]GTP1 or [^{18}F]florbetapir SUVR across the entire study population

Tracer	MMSE		CDR-SB		ADAS-Cog13		Total RBANS	
	r_s	p	r_s	p	r_s	p	r_s	p
[^{18}F]GTP1								
WCG	−0.49	<0.001	0.53	<0.001	0.59	<0.001	−0.63	<0.001
Temporal meta-ROI	−0.58	<0.001	0.60	<0.001	0.70	<0.001	−0.72	<0.001
[^{18}F]florbetapir								
WCG	−0.33	0.006	0.39	0.001	0.35	0.003	−0.41	0.001
Temporal meta-ROI	−0.22	0.073	0.23	0.055	0.22	0.077	−0.35	0.005

Key: AD = Alzheimer's Disease; ADAS-Cog13 = 13-item version of the Alzheimer's Disease Assessment Scale–Cognitive Subscale; CDR-SB = Clinical Dementia Rating Sum of Boxes; MMSE = Mini–Mental State Examination; RBANS = Repeatable Battery for the Assessment of Neuropsychological Status; ROI = region of interest; SUVR = standardized uptake value ratio; WCG = whole cortical gray matter.

demonstrating a significant overall relationship between [^{18}F]florbetapir SUVR and cognition. Therefore, we repeated the analyses using only the AD participants (Supplemental Table 1). All of the correlations between [^{18}F]GTP1 SUVR and the global cognitive indices remained significant (all $p < 0.005$). However, for [^{18}F]florbetapir SUVR, only the correlation with total RBANS score remained significant ($p = 0.031$). Likewise, partial correlation analyses demonstrated that all of the [^{18}F]GTP1 SUVR/cognition correlations survived adjustment for Aβ signal, but the [^{18}F]florbetapir SUVR/total RBANS correlation did not survive adjustment for tau signal (Supplementary Fig. 2).

3.4. Correlations between AD meta-ROI [^{18}F]GTP1 SUVR and cognition

Prior work with [^{18}F]flortaucipir tau PET suggests that SUVRs calculated from a temporal meta-ROI efficiently distinguish AD participants from CN controls (Jack et al., 2017) because of preferential deposition of tau pathology in temporal lobe regions, particularly at earlier stages of AD. When we investigated associations between cognition and [^{18}F]GTP1 SUVR in this more AD-specific region, our analyses demonstrated numerically larger correlation coefficients with the temporal meta-ROI relative to the WCG ROI (Table 2). Notably, when associations between cognition and [^{18}F]florbetapir SUVR were examined, an opposite trend toward numerically smaller correlation coefficients was seen with the temporal meta-ROI relative to the WCG ROI (Table 2).

3.5. Multiple linear regression of cognition and [^{18}F]GTP1 SUVR, [^{18}F]florbetapir SUVR, cortical volume, and age

Because tau pathology, Aβ pathology, brain atrophy, and age may each contribute to cognitive performance in an independent and/or interrelated fashion (Bejanin et al., 2017), we performed further multiple linear regression analyses to determine the relative associations between each global cognitive measure, imaging indices ([^{18}F]GTP1 SUVR, [^{18}F]florbetapir SUVR, and cortical volume measured by MRI, each using the temporal meta-ROI), and age (Table 3). These analyses indicated that while [^{18}F]GTP1 SUVR and cortical volumes were consistently significantly correlated with baseline cognitive performance in an independent fashion, age and [^{18}F]florbetapir SUVR were not. A similar (although less robust) overall pattern of results emerged when these analyses were performed using WCG imaging indices (Supplemental Table 2).

3.6. Correlations between individual RBANS subtests and [^{18}F]GTP1 SUVR in individual ROIs

Recent work with [^{18}F]flortaucipir PET imaging in cohorts that included significant proportions of patients with atypical focal cortical AD variants indicated that different patterns of regional tau deposition in AD correlate with deficits in different cognitive domains (Bejanin et al., 2017; Ossenkoppele et al., 2016). However, in such focal cortical AD variants, tau pathology (Mesulam et al., 2008, 2014; Tang-Wai et al., 2004) and cortical atrophy (Josephs et al., 2013; Lehmann et al., 2011; Madhavan et al., 2013; Peng et al., 2016; Whitwell et al., 2007) exhibit topographic patterns that diverge from those seen in more typical amnestic-onset AD. These more focal patterns of pathology may contribute to stronger correlations between regional tau PET signal and specific domains of cognitive performance relative to the broader AD population.

To determine whether similar correlations might emerge with [^{18}F]GTP1 PET imaging in our cohort, which was not enriched with participants with atypical focal cortical AD syndromes, we examined associations between performance on individual RBANS subtests and [^{18}F]GTP1 SUVR in individual Hammers atlas ROIs averaged across the left and right hemispheres. Fig. 2 illustrates Spearman correlations between individual ROIs and subtests using a heat map representation. More detailed statistical results from these exploratory analyses are shown in Supplementary Fig. 3 and Supplementary Table 3.

Across most items, larger correlation coefficients were most consistently observed in the temporal lobe, reflecting the early and hierarchical deposition of tau pathology in sporadic late-onset AD

Table 3
Results of multiple linear regression analyses regressing cognitive indices against demographic and imaging variables (using the temporal meta-ROI)

Covariate	MMSE $r^2 = 0.51$		CDR-SB $r^2 = 0.50$		ADAS-Cog13 $r^2 = 0.55$		RBANS $r^2 = 0.56$	
	B (SE)	t	B (SE)	t	B (SE)	t	B (SE)	t
Age (10 y)	0.09 (0.71)	0.13	0.40 (0.39)	1.03	1.21 (1.67)	0.72	1.84 (2.19)	0.84
[^{18}F]GTP1 (0.1 SUVR)	−0.65 (0.20)	−3.35[a]	0.27 (0.11)	2.48[a]	1.66 (0.46)	3.60[a]	−2.02 (0.63)	−3.19[a]
Volumetric MRI (cm^3)	0.23 (0.07)	3.34[a]	−0.14 (0.04)	−3.65[a]	−0.53 (0.16)	−3.28[a]	0.98 (0.23)	4.35[a]
[^{18}F]florbetapir (0.1 SUVR)	0.17 (0.37)	0.45	−0.18 (0.20)	−0.87	−0.56 (0.86)	−0.65	−1.33 (1.15)	−1.16

Partial regression coefficients (B), standard errors (SE), and t statistics are reported for each predictor; r^2 values are reported for each multiple regression model.
Key: ADAS-Cog13 = 13-item versions of the Alzheimer's Disease Assessment Scale-Cognitive Subscale; CDR-SB = Clinical Dementia Rating Sum of Boxes; MRI = magnetic resonance imaging; MMSE = Mini–Mental State Examination; RBANS = Repeatable Battery for the Assessment of Neuropsychological Status; SUVR = standardized uptake value ratio.
[a] $p < 0.05$.

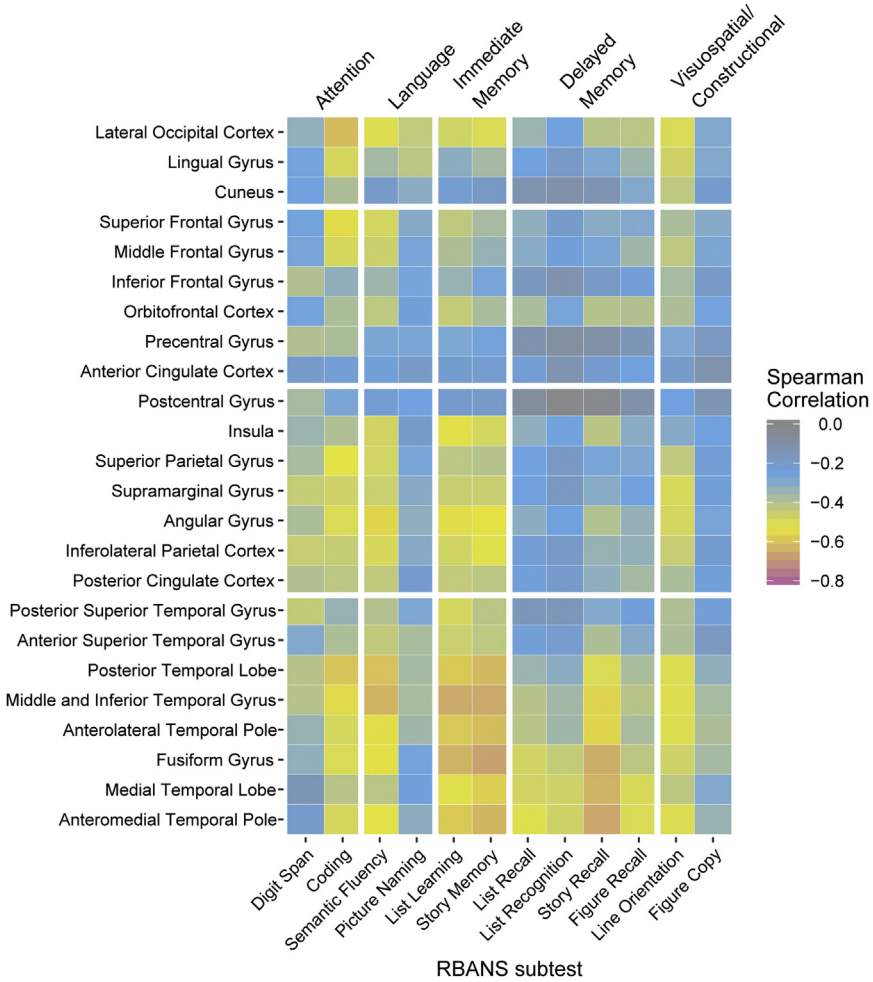

Fig. 2. Heat map of Spearman's correlations between [^{18}F]GTP1 SUVR in individual Hammers Atlas ROIs averaged across the left and right hemispheres and performance on individual RBANS subtests. Abbreviations: ROIs = regions of interest; RBANS = Repeatable Battery for the Assessment of Neuropsychological Status; SUVR = standardized uptake value ratio.

in this region (Braak and Braak, 1991). Poorer performance on delayed memory subtests showed more specific associations with [^{18}F]GTP1 SUVR in temporal lobe ROIs, whereas poorer performance on other RBANS subtests also showed a broader range of larger correlation coefficients with [^{18}F]GTP1 SUVR with ROIs in other areas. Analyses performed using only left or right hemisphere ROIs yielded similar overall patterns of results (Supplemental Fig. 4). However, there was a suggestion of asymmetry in the magnitude of correlation coefficients for associations between [^{18}F]GTP1 SUVR and performance on language (left > right) and visuospatial (right > left) subtests, which is consistent with prior work on brain-behavior relationships focused on hemispheric specialization (Lezak et al., 2004).

4. Discussion

Our results demonstrate that [^{18}F]GTP1 PET signal in a cohort of participants with normal cognition through moderate AD dementia significantly correlates with cognitive performance across multiple measures. In particular, tau pathology and cortical volume (but not Aβ pathology) were independently associated with performance on global cognitive indices. These findings reinforce prior [^{18}F]flortaucipir data suggesting that cognitive deficits in AD could arise both directly from tau pathology and from subsequent downstream cortical atrophy (Bejanin et al., 2017).

Although these correlations are apparent when [^{18}F]GTP1 PET signal is averaged across the WCG, previous work has shown that tau PET signal, particularly at earlier stages of AD progression, is concentrated in the temporal lobes (Cho et al., 2016; Jack et al., 2017; Mattsson et al., 2017; Pontecorvo et al., 2017; Sanabria-Bohorquez et al., 2019; Schwarz et al., 2016). Correspondingly, the magnitude of the correlations between cognitive indices and [^{18}F]GTP1 PET signal became numerically larger when a temporal lobe meta-ROI was used. Although these findings arise in part from the hierarchical topography of tau deposition in AD in less-advanced disease (Braak and Braak, 1991), they also likely reflect the predominance of memory-related items in commonly used cognitive assessments for AD. Indeed, 45/85 possible points on the ADAS-Cog13, 16/30 possible points on the MMSE, and 6/18 possible points on the CDR-SB are explicitly related to immediate or delayed memory and orientation. Likewise, 6/12 RBANS subtests assess learning, recall, or recognition of verbal or visuospatial information. Furthermore, the emphasis on amnestic AD in the inclusion criteria for this study may have also contributed to the strength of these associations.

The relative strength of the relationship between temporal lobe tau PET signal and memory function, particularly verbal memory,

can be seen in the heat map of correlations between individual subtests of the RBANS and individual Hammers atlas ROIs (Fig. 2). Overall, our results are consistent with prior analyses of correlations between temporal lobe [^{18}F]flortaucipir PET signal and memory function in both CN older controls (Maass et al., 2018; Schöll et al., 2016) and participants with mild cognitive impairment or AD dementia (Bejanin et al., 2017; Cho et al., 2016; Schwarz et al., 2016). Taken together, these results suggest that temporal lobe uptake of either [^{18}F]GTP1 or [^{18}F]flortaucipir accurately represents the in vivo tau burden that contributes to memory deficits in AD.

However, our results do not fully recapitulate prior [^{18}F]flortaucipir PET results from two overlapping cohorts that suggested distinctly different patterns of correlation between regional localization of tau deposition and performance on language and visuospatial assessments (Bejanin et al., 2017; Ossenkoppele et al., 2016). In particular, regional correlations between [^{18}F]GTP1 SUVR and performance on language and visuospatial RBANS subtests in the present cohort were less well circumscribed (Fig. 2 and Supplemental Fig. 3). There are a number of potential explanations for these discordant results. The previously reported cohorts included more participants with atypical focal cortical AD variants (e.g., logogenic progressive aphasia, posterior cortical atrophy) who may exhibit more circumscribed and distinct distributions of tau pathology relative to more common amnestic presentations (Mesulam et al., 2008, 2014; Tang-Wai et al., 2004). While RBANS subtests (Randolph et al., 1998) are designed to assess neuropsychological constructs similar to those assessed by the longer neuropsychological battery used in previous studies (Bejanin et al., 2017; Ossenkoppele et al., 2016), domain-specific composite scores derived from the previous battery may be more sensitive to deficits resulting from regional deposition of tau neuropathology. Conversely, the focus on amnestic AD in the present study may have contributed to our finding of stronger regional correlations between memory function and [^{18}F]GTP1 signal relative to other cognitive domains. Because the primary aim of the study through which the cognitive data included in our analyses were obtained was to characterize longitudinal changes in [^{18}F]GTP1 imaging indices, data collection for participants' level of education was not included in the study protocol, which precludes adjustments for this potential proxy of cognitive reserve. Finally, while these data represent the largest analysis of the relationships between [^{18}F]GTP1 imaging and cognitive indices to date, the relatively homogenous racial/ethnic background of our participants and the relatively smaller sample sizes within individual diagnostic groups may limit the interpretation of our results.

Although our work further establishes the cross-sectional relationship between tau PET signal and cognitive function in AD, associations between baseline levels and longitudinal increases in tau PET signal versus longitudinal declines in cognitive function have yet to be explored in detail. Recent work suggests tau PET may have utility as a prognostic biomarker, as higher baseline SUVRs are associated with greater subsequent cognitive decline (Koychev et al., 2017; Mintun et al., 2017; Teng et al., 2018). In addition, longitudinal data from cognitively impaired Aβ-positive participants enrolled in the Mayo Clinic Study of Aging show that [^{18}F]flortaucipir signal significantly increases over 12–15 months (Jack et al., 2018). Because tau PET has now been integrated into several other ongoing longitudinal observational studies that include participants with AD, such as ADNI3, BioFINDER, and AIBL (Brown et al., 2018; Hansson et al., 2017), further elucidation of the associations between changes in longitudinal tau PET and cognition should be shortly forthcoming. Furthermore, because tau PET imaging has also been incorporated into several therapeutic studies in AD that use anti-Aβ (solanezumab [NCT02008357], crenezumab [NCT02670083, NCT03114657], and gantenerumab [NCT03443973, NCT03444870]) or anti-tau (RO7105705 [NCT03289143], ABBV-8E12 [NCT02880956], and BIIB092/BMS-986168 [NCT03352557]) interventions, the potential of this tau biomarker modality as a predictive, prognostic, and/or surrogate biomarker for clinical AD progression should be further clarified in the near future.

Disclosure

All authors are current or former employees or contractors of Genentech, Inc. All authors except RDR and SB are current or former shareholders of F. Hoffmann La Roche, Ltd.

Acknowledgements

This work was supported by Genentech, Inc., employees of which participated in design and conduct of the study; collection, management, analysis, and interpretation of the data, preparation, review, or approval of the manuscript, and decision to submit the manuscript for publication. The authors would like to thank all of the study participants and their families, and all of the site investigators, study coordinators, and staff. Writing assistance was provided by B. Hains, PhD at Genentech, Inc.

Appendix A. Supplementary data

Supplementary data to this article can be found online at https://doi.org/10.1016/j.neurobiolaging.2019.05.026.

References

Albert, M., DeKosky, S., Dickson, D., Dubois, B., Feldman, H.H., Fox, N.C., Gamst, A., Holtzman, D.M., Jagust, W.J., Petersen, R.C., Snyder, P.J., Carrillo, M.C., Thies, B., Phelps, C.H., 2011. The diagnosis of mild cognitive impairment due to Alzheimer's disease: recommendations from the National Institute on Aging-Alzheimer's Association workgroups on diagnostic guidelines for Alzheimer's disease. Alzheimers Dement. 7, 270–279.

Bejanin, A., Schonhaut, D.R., La Joie, R., Kramer, J.H., Baker, S.L., Sosa, N., Ayakta, N., Cantwell, A., Janabi, M., Lauriola, M., O'Neil, J.P., Gorno-Tempini, M.L., Miller, Z.A., Rosen, H.J., Miller, B.L., Jagust, W.J., Rabinovici, G.D., 2017. Tau pathology and neurodegeneration contribute to cognitive impairment in Alzheimer's disease. Brain 140, 3286–3300.

Blennow K., Chen, C., Cicognola, C., Wildsmith, K.R., Manser, P.T., Sanabria-Bohorquez, S., Zheng, Z., Xie, B., Peng, J., Hansson, O., Kvartsberg, H., Portelius, E., Zetterberg, H., Lashley, T., Brinkmalm G., Kerchner, G.A., Weimer R.M., Ye, K., Hoglund K., submitted. Cerebrospinal fluid levels of a tau fragment ending at amino acid 368 correlate with tau PET: a candidate biomarker for tangle pathology in Alzheimer's disease. Brain.

Braak, H., Braak, E., 1991. Neuropathological stageing of Alzheimer-related changes. Acta Neuropathol. 82, 239–259.

Brier, M.R., Gordon, B., Friedrichsen, K., McCarthy, J., Stern, A., Christensen, J., Owen, C., Aldea, P., Su, Y., Hassenstab, J., Cairns, N.J., Holtzman, D.M., Fagan, A.M., Morris, J.C., Benzinger, T.L., Ances, B.M., 2016. Tau and Aβ imaging, CSF measures, and cognition in Alzheimer's disease. Sci. Transl. Med. 8, 338ra66.

Brown, B.M., Rainey-Smith, S.R., Dore, V., Peiffer, J.J., Burnham, S.C., Laws, S.M., Taddei, K., Ames, D., Masters, C.L., Rowe, C.C., Martins, R.N., Villemagne, V.L., 2018. Self-reported physical activity is associated with tau burden measured by positron emission tomography. J. Alzheimers Dis. 63, 1299–1305.

Cho, H., Choi, J.Y., Hwang, M.S., Lee, J.H., Kim, Y.J., Lee, H.M., Lyoo, C.H., Ryu, Y.H., Lee, M.S., 2016. Tau PET in Alzheimer disease and mild cognitive impairment. Neurology 87, 375–383.

Folstein, M.F., McHugh, P.R., 1975. Mini-mental state. A practical method for grading the cognitive state of patients for the clinician. J. Psychol. Res. 12, 189–198.

Hammers, A., Allom, R., Koepp, M.J., Free, S.L., Myers, R., Lemieux, L., Mitchell, T.N., Brooks, D.J., Duncan, J.S., 2003. Three-dimensional maximum probability atlas of the human brain, with particular reference to the temporal lobe. Hum. Brain Mapp. 19, 224–247.

Hansson, O., Grothe, M.J., Strandberg, T.O., Ohlsson, T., Hägerström, D., Jögi, J., Smith, R., Schöll, M., 2017. Tau pathology distribution in Alzheimer's disease corresponds differentially to cognition-relevant functional brain networks. Front. Neurosci. 11, 167.

Jack, C.R., Wiste, H.J., Weigand, S.D., Therneau, T.M., Lowe, V.J., Knopman, D.S., Gunter, J.L., Senjem, M.L., Jones, D.T., Kantarci, K., Machulda, M.M., Mielke, M.M., Roberts, R.O., Vemuri, P., Reyes, D.A., Petersen, R.C., 2017. Defining imaging

biomarker cut points for brain aging and Alzheimer's disease. Alz. Demen. 13, 205–216.
Jack Jr., C.R., Wiste, H.J., Schwarz, C.G., Lowe, V.J., Senjem, M.L., Vemuri, P., Weigand, S.D., Therneau, T.M., Knopman, D.S., Gunter, J.L., Jones, D.T., Graff-Radford, J., Kantarci, K., Roberts, R.O., Mielke, M.M., Machulda, M.M., Petersen, R.C., 2018. Longitudinal tau PET in ageing and Alzheimer's disease. Brain 141, 1517–1528.
Johnson, K.A., Schultz, A., Betensky, R.A., Becker, J.A., Sepulcre, J., Rentz, D., Mormino, E., Chhatwal, J., Amariglio, R., Papp, K., Marshall, G., Albers, M., Mauro, S., Pepin, L., Alverio, J., Judge, K., Philiossaint, M., Shoup, T., Yokell, D., Dickerson, B., Gomez-Isla, T., Hyman, B., Vasdev, N., Sperling, R., 2016. Tau positron emission tomographic imaging in aging and early Alzheimer disease. Ann. Neurol. 79, 110–119.
Josephs, K.A., Dickson, D.W., Murray, M.E., Senjem, M.L., Parisi, J.E., Petersen, R.C., Jack Jr., C.R., Whitwell, J.L., 2013. Quantitative neurofibrillary tangle density and brain volumetric MRI analyses in Alzheimer's disease presenting as logopenic progressive aphasia. Brain Lang. 127, 127–134.
Joshi, A.D., Pontecorvo, M.J., Clark, C.M., Carpenter, A.P., Jennings, D.L., Sadowsky, C.H., Adler, L.P., Kovnat, K.D., Seibyl, J.P., Arora, A., Saha, K., Burns, J.D., Lowrey, M.J., Mintun, M.A., Skovronsky, D.M., Florbetapir F 18 Study Investigators, 2012. Performance characteristics of amyloid PET with florbetapir F 18 in patients with Alzheimer's disease and cognitively normal subjects. J. Nucl. Med. 53, 378–384.
Koychev, I., Gunn, R.N., Firouzian, A., Lawson, J., Zamboni, G., Ridha, B., Sahakian, B.J., Rowe, J.B., Thomas, A., Rochester, L., Ffytche, D., Howard, R., Zetterberg, H., MacKay, C., Lovestone, S., Deep and Frequent Phenotyping study team, 2017. PET tau and amyloid-β burden in mild Alzheimer's disease: divergent relationship with age, cognition, and cerebrospinal fluid biomarkers. J. Alzheimers Dis. 60, 283–293.
La Joie, R., Bejanin, A., Fagan, A.M., Ayakta, N., Baker, S.L., Bourakova, V., Boxer, A.L., Cha, J., Karydas, A., Jerome, G., Maass, A., Mensing, A., Miller, Z.A., O'Neil, J.P., Pham, J., Rosen, H.J., Tsai, R., Visani, A.V., Miller, B.L., Jagust, W.J., Rabinovici, G.D., 2018. Associations between [(18)F]AV1451 tau PET and CSF measures of tau pathology in a clinical sample. Neurology 90, e282–e290.
Lehmann, M., Crutch, S.J., Ridgway, G.R., Ridha, B.H., Barnes, J., Warrington, E.K., Rossor, M.N., Fox, N.C., 2011. Cortical thickness and voxel-based morphometry in posterior cortical atrophy and typical Alzheimer's disease. Neurobiol. Aging 32, 1466–1476.
Lezak, M.D., Howieson, D.B., Loring, D.W., Hannay, H.J., Fischer, J.S., 2004. Neuropsychological Assessment, fourth ed. Oxford University Press, New York, NY, US.
Maass, A., Lockhart, S.N., Harrison, T.M., Bell, R.K., Mellinger, T., Swinnerton, K., Baker, S.L., Rabinovici, G.D., Jagust, W.J., 2018. Entorhinal tau pathology, episodic memory decline, and neurodegeneration in aging. J. Neurosci. 38, 530–543.
Madhavan, A., Whitwell, J.L., Weigand, S.D., Duffy, J.R., Strand, E.A., Machulda, M.M., Tosakulwong, N., Senjem, M.L., Gunter, J.L., Lowe, V.J., Petersen, R.C., Jack Jr., C.R., Josephs, K.A., 2013. FDG PET and MRI in logopenic primary progressive aphasia versus dementia of the Alzheimer's type. PLoS One 8, e62471.
Mattsson, N., Schöll, M., Strandberg, O., Smith, R., Palmqvist, S., Insel, P.S., Hägerström, D., Ohlsson, T., Zetterberg, H., Jögi, J., Blennow, K., Hansson, O., 2017. (18)F-AV-1451 and CSF T-tau and P-tau as biomarkers in Alzheimer's disease. EMBO Mol. Med. 9, 1212–1223.
McKhann, G.M., Knopman, D.S., Chertkow, H., Hyman, B.T., Jack Jr., C.R., Kawas, C.H., Klunk, W.E., Koroshetz, W.J., Manly, J.J., Mayeux, R., Mohs, R.C., Morris, J.C., Rossor, M.N., Scheltens, P., Carrillo, M.C., Thies, B., Weintraub, S., Phelps, C.H., 2011. The diagnosis of dementia due to Alzheimer's disease: recommendations from the National Institute on Aging-Alzheimer's Association workgroups on diagnostic guidelines for Alzheimer's disease. Alz. Demen. 7, 263–269.
Mesulam, M., Wicklund, A., Johnson, N., Rogalski, E., Léger, G.C., Rademaker, A., Weintraub, S., Bigio, E.H., 2008. Alzheimer and frontotemporal pathology in subsets of primary progressive aphasia. Ann. Neurol. 63, 709–719.
Mesulam, M.M., Weintraub, S., Rogalski, E.J., Wieneke, C., Geula, C., Bigio, E.H., 2014. Asymmetry and heterogeneity of Alzheimer's and frontotemporal pathology in primary progressive aphasia. Brain 137, 1176–1192.
Mintun, M.A., Devous, M.D., Lu, M., 2017. PET biomarkers in the EXPEDITION 3 trial of patients with mild AD. Alz. Demen. 13, P1452.
Mohs, R.C., Knopman, D., Petersen, R.C., Ferris, S.H., Ernesto, C., Grundman, M., Sano, M., Bieliauskas, L., Geldmacher, D., Clark, C., Thal, L.J., 1997. Development of cognitive instruments for use in clinical trials of antidementia drugs: additions to the Alzheimer's Disease Assessment Scale that broaden its scope. The Alzheimer's Disease Cooperative Study. Alzheimer Dis. Assoc. Disord. 11 (Suppl 2), S13–S21.
Morris, J., 1997. Clinical dementia rating: a reliable and valid diagnostic and staging measure for dementia of the Alzheimer type. Int. Psychogeriatr. 9, 173–176.
Nelson, P.T., Alafuzoff, I., Bigio, E.H., Bouras, C., Braak, H., Cairns, N.J., Castellani, R.J., Crain, B.J., Davies, P., Del Tredici, K., Duyckaerts, C., Frosch, M.P., Haroutunian, V., Hof, P.R., Hulette, C.M., Hyman, B.T., Iwatsubo, T., Jellinger, K.A., Jicha, G.A., Kövari, E., Kukull, W.A., Leverenz, J.B., Love, S., Mackenzie, I.R., Mann, D.M., Masliah, E., McKee, A.C., Montine, T.J., Morris, J.C., Schneider, J.A., Sonnen, J.A., Thal, D.R., Trojanowski, J.Q., Troncoso, J.C., Wisniewski, T., Woltjer, R.L., Beach, T.G., 2012. Correlation of Alzheimer disease neuropathologic changes with cognitive status: a review of the literature. J. Neuropath. Exp. Neurol. 71, 362–381.
Ossenkoppele, R., Schonhaut, D.R., Schöll, M., Lockhart, S.N., Ayakta, N., Baker, S.L., O'Neil, J.P., Janabi, M., Lazaris, A., Cantwell, A., Vogel, J., Santos, M., Miller, Z.A., Bettcher, B.M., Vossel, K.A., Kramer, J.H., Gorno-Tempini, M.L., Miller, B.L., Jagust, W.J., Rabinovici, G.D., 2016. Tau PET patterns mirror clinical and neuroanatomical variability in Alzheimer's disease. Brain 139, 1551–1567.
Peng, G., Wang, J., Feng, Z., Liu, P., Zhang, Y., He, F., Chen, Z., Zhao, K., Luo, B., 2016. Clinical and neuroimaging differences between posterior cortical atrophy and typical amnestic Alzheimer's disease patients at an early disease stage. Sci. Rep. 6, 29372.
Pontecorvo, M.J., Devous, M.D., Navitsky, M., Lu, M., Salloway, S., Schaerf, F.W., Jennings, D., Arora, A.K., McGeehan, A., Lim, N.C., Xiong, H., Joshi, A.D., Siderowf, A., Mintun, M.A., 18F-AV-1451-A05 investigators, 2017. Relationships between flortaucipir PET tau binding and amyloid burden, clinical diagnosis, age and cognition. Brain 140, 748–763.
Querfurth, H.W., LaFerla, F.M., 2010. Alzheimer's disease. N. Engl. J. Med. 362, 329–344.
R Core Team, 2016. R: A Language and Environment for Statistical Computing. R Foundation for Statistical Computing, Vienna, Austria. http://www.R-project.org/. (Accessed 25 June 2019).
Randolph, C., Tierny, M.C., Mohr, C., Chase, T.C., 1998. The repeatable battery for the assessment of neuropsychological status (RBANS): preliminary clinical validity. J. Clin. Exp. Neuropsychol. 20, 310–319.
Sanabria-Bohorquez, S., Marik, J., Ogasawara, A., Tinianow, J.N., Gill, H.S., Barret, O., Tamagnan, G., Alagille, D., Ayalon, G., Manser, P., Bengtsson, T., Ward, M., Williams, S.P., Kerchner, G.A., Seibyl, J.P., Marek, K., Weimer, R.M., 2019. In revision. First-in-human evaluation of [18F]GTP1 (Genentech Tau Probe 1), a radioligand for detecting neurofibrillary tangle tau pathology in Alzheimer's disease. Eur. J. Nucl. Med. Mol. Imaging 46, 2077–2089.
Schöll, M., Lockhart, S.N., Schonhaut, D.R., O'Neil, J.P., Janabi, M., Ossenkoppele, R., Baker, S.L., Vogel, J.W., Faria, J., Schwimmer, H.D., Rabinovici, G.D., Jagust, W.J., 2016. PET Imaging of tau deposition in the aging human brain. Neuron 89, 971–982.
Schwarz, A.J., Yu, P., Miller, B.B., Shcherbinin, S., Dickson, J., Navitsky, M., Joshi, A.D., Devous, M.D., Mintun, M.S., 2016. Regional profiles of the candidate tau PET ligand 18F-AV-1451 recapitulate key features of Braak histopathological stages. Brain 139, 1539–1550.
Tang-Wai, D.F., Graff-Radford, N.R., Boeve, B.F., Dickson, D.W., Parisi, J.E., Crook, R., Caselli, R.J., Knopman, D.S., Petersen, R.C., 2004. Clinical, genetic, and neuropathologic characteristics of posterior cortical atrophy. Neurology 63, 1168–1174.
Teng, E., Manser, P.T., Ward, M., Sanabria-Bohorquez, S., Ray, R., Baker, S.L., Kerchner, G.A., Weimer, R., 2018. Baseline tau burden measured by [^{18}F]GTP1 imaging is associated with subsequent cognitive decline in prodromal to mild Alzheimer's disease. Alz. Demen. 14, P1604–P1605.
Villemagne, V.L., Doré, V., Burnham, S.C., Masters, C.L., Rowe, C.C., 2018. Imaging tau and amyloid-β proteinopathies in Alzheimer disease and other conditions. Nat. Rev. Neurol. 14, 225–236.
Whitwell, J.L., Jack Jr., C.R., Kantarci, K., Weigand, S.D., Boeve, B.F., Knopman, D.S., Drubach, D.A., Tang-Wai, D.F., Petersen, R.C., Josephs, K.A., 2007. Imaging correlates of posterior cortical atrophy. Neurobiol. Aging 28, 1051–1061.